Materials Science & Engineering A 734 (2018) 281–290

Contents lists available at ScienceDirect

Materials Science & Engineering A

journal homepage: www.elsevier.com/locate/msea

Micromechanics and microstructure evolution during *in situ* uniaxial tensile loading of TRIP-assisted duplex stainless steels

Ye Tian[a,*], Sen Lin[a], J.Y. Peter Ko[b], Ulrich Lienert[c], Annika Borgenstam[a], Peter Hedström[a]

[a] Department of Materials Science and Engineering, KTH Royal Institute of Technology, Stockholm SE-10044, Sweden
[b] Cornell High Energy Synchrotron Source, Cornell University, Ithaca, NY 14853, United States
[c] Deutsches Elektronen-Synchrotron, DESY Photon Science, Hamburg 22607, Germany

ARTICLE INFO

Keywords:
Synchrotron x-ray diffraction
in situ tensile loading
Duplex stainless steel
Load partitioning
TRIP-assisted steel
Micromechanics

ABSTRACT

Transformation-induced plasticity (TRIP) assisted duplex stainless steels, with three different stabilities of the austenite phase, were investigated by synchrotron x-ray diffraction characterization during *in situ* uniaxial tensile loading. The micromechanics and the deformation-induced martensitic transformation (DIMT) in the bulk of the steels were investigated *in situ*. Furthermore, scanning electron microscopy supplemented the *in situ* analysis by providing information about the microstructure of annealed and deformed specimens. The dependence of deformation structure on austenite stability is similar to that of single-phase austenitic steels with shear bands and *bcc*-martensite (α') generally observed, and blocky α' is only frequent when the austenite stability is low. These microstructural features, i.e. defect structure and deformation-induced martensite, are correlated with the micro- and macro-mechanics of the steels with elastoplastic load transfer from the weaker phases to the stronger α', in particular this occurs close to the point of maximum rate of α' formation. A clear strain-hardening effect from α' is seen in the most unstable austenite leading to a pronounced TRIP effect.

1. Introduction

Duplex stainless steels constitute of a mixture of approximately equal amounts of the austenite and ferrite phases (hereinafter referred to as γ and α, respectively). They have good corrosion resistance and mechanical properties with, in general, yield strength superior, but ductility inferior, to austenitic grades. The duplex stainless steels find frequent use in storage containers and piping, especially in harsh environments and in conditions where austenitic grades would be susceptible to stress corrosion [1]. Recently, there has been a development effort aimed at increasing the ductility and formability of the duplex stainless steels. In designing these alloy, the transformation-induced plasticity (TRIP) phenomenon has been utilized by tuning the γ stability via suitable alloying additions. The TRIP effect is achieved by deformation-induced martensitic transformation (DIMT), providing additional work hardening that postpones plastic instability and necking. The TRIP effect is successfully utilized in numerous steels, not only in these duplex steels, but also in metastable austenitic stainless steels, TRIP carbon steels [2], quenching & partitioning steels [3], maraging steels [4] and other high strength steels [5–7]. The new TRIP-assisted duplex stainless steels investigated here and hereinafter referred to as TDSS, can have total elongations over ~ 60% and ultimate tensile strengths up to ~1 GPa [8].

The deformation behaviour of the conventional duplex stainless steels is complex and the interplay between γ and α has been studied extensively using *in situ* x-ray and neutron diffraction experiments [9–13]. The inhomogeneous deformation behaviour with load partitioning between the phases [9], textural components [12] and grains [11] has been documented. The TDSS are, however, even more complex due to the possible transformation of the metastable austenite to two kinds of products, i.e. *hcp*- and *bcc*-martensite (hereinafter referred to as ε and α', respectively), during deformation. Many previous studies on DIMT have been devoted to the investigation of TRIP carbon steels [2,4,14–16] and metastable austenitic stainless steels [17–20], but studies of DIMT in TDSS are rarely presented, apart from some recent reports [8,21–23].

A better understanding of the deformation behaviour of TDSS is necessary in order to continue to improve and optimize their mechanical properties. It is known from other TRIP-assisted multiphase steels that their mechanical behaviour can be largely influenced by the γ stability [15,24–26], and that their mechanical response is attributed also to effects such as defect formation and load redistribution between phases and grains [22,26]. However, the available reports for TDSS have mainly focused on the DIMT itself [21–23,27] instead of the more

* Corresponding author.
E-mail address: yti@kth.se (Y. Tian).

https://doi.org/10.1016/j.msea.2018.07.040
Received 22 March 2018; Received in revised form 10 July 2018; Accepted 11 July 2018

Table 1
Chemical compositions of the investigated steels (wt%).

	C	Si	Mn	Cr	Ni	Mo	Ti	Al
FDX25	0.023	0.38	2.52	20.26	1.48	0.4	0.001	0.009
FDX27	0.021	0.38	0.93	19.97	3.05	1.15	0.003	0.02

	Nb	Cu	Co	N	W	V	Fe
FDX25	0.004	0.5	0.04	0.22	< 0.01	0.06	Bal.
FDX27	0.004	0.32	0.06	0.18	0.01	0.06	Bal.

complete view of the deformation behaviour due to microstructure evolution and micromechanics.

The aim of the present work is to study the deformation behaviour of two TDSS with different γ stability and, furthermore, to investigate the effect of increasing temperature on deformation in one of the steels. High-energy x-ray diffraction (HEXRD) measurements during *in situ* uniaxial tensile loading are applied to study the micromechanics and DIMT. It is further supplemented by electron microscopy investigations.

2. Experimental methods

2.1. Materials

The experiments were carried out on two TDSS, FDX27 and FDX25, supplied by Outokumpu Stainless. The as-received state was 1 mm thick steel sheets with the chemical compositions given in Table 1. Both steels were tested at room temperature (RT) and, FDX25 was also tested at 45 °C. The testing conditions are hereinafter referred to as FDX27@RT, FDX25@RT and FDX25@45. Dog-bone-shaped tensile specimens with a gauge length of 3 mm and gauge width of 1 mm, shown in the upper left corner of Fig. 1, were cut from the steel sheets using electrical discharge machining. The specimens were then ground and polished to a final thickness of 0.8 mm. In the grip section of the specimens, two holes were drilled for pin-hole attachment in the tensile rig.

2.2. In situ loading experiments

2.2.1. High-energy x-ray diffraction measurements during in situ tensile loading

In situ uniaxial tensile loading experiments were performed in a customized load frame, called rotational and axial motion system (RAMS) dedicated for HEXRD experiments, which is shown in Fig. 1. A detailed description of the RAMS can be found in Shade et al. [28]. During tensile tests at 45 °C the temperature was regulated by a furnace containing halogen bulbs and an elliptical mirror to focus the light onto the specimen. Two thermocouples were used for furnace control and two for specimen temperature measurements. The load was applied along the rolling direction of the sheet steel, and measured using a load cell with a 2 kN capacity. Interrupted tensile loading was performed using displacement control at a strain rate of 5×10^{-4} s^{-1} up to an applied logarithmic strain of 0.26 (evaluated via the displacement of the load frame). HEXRD measurements were performed *in situ* during loading. The experiments were conducted at the F2 beamline at the Cornell High Energy Synchrotron Source (CHESS), U.S, using an x-ray beam with an energy of 61.332 keV (0.20218 Å), collimated to a size of $0.8 \times 2\,mm^2$ (V × H). An area detector (GE Detector 2048 × 2048 pixels, 200 × 200 μm^2 per pixel) was placed about 1012 mm behind the specimen to collect the diffraction patterns. For each strain step, a 2D diffraction pattern was acquired for a constant ω angle of 0° (incoming beam parallel to specimen's normal direction). The 2-theta (2θ) angle is in the radial direction of the detector. Prior to the *in situ* experiments a standard CeO_2 powder specimen was measured for calibration purposes.

2.2.2. Data analysis for phase quantification

The 2D diffraction data was calibrated and processed using mainly the GSAS-II software [29], and the patterns acquired during the *in situ* experiments were integrated over 360° in the azimuthal direction (η). Fitting of the peaks was performed by a combination of single-peak and multiple-peak fitting. This procedure enabled good fitting for all peaks, even for low intensity peaks from the ε phase. Fig. 2a shows an example of the raw 2D pattern, Fig. 2b shows the overview of integrated 1D patterns and Fig. 2c shows the least-squares fitting of peaks using pseudo-Voigt functions.

The direct comparison method [30] was used to determine the volume fractions of the phases. This methodology is intended for powder patterns, assuming a random texture, but it is also known that by measuring multiple orientations and peaks for each phase the effect of texture on phase quantification will be minimized [31]. The volume fraction is evaluated using:

$$V_i = \left(\frac{1}{n}\sum_{j=1}^{n}\frac{I_i^j}{R_i^j}\right) \Big/ \left(\frac{1}{p}\sum_{k=1}^{p}\frac{I_\gamma^k}{R_\gamma^j} + \frac{1}{q}\sum_{l=1}^{q}\frac{I_\varepsilon^l}{R_\varepsilon^l} + \frac{1}{r}\sum_{m=1}^{r}\frac{I_{bcc}^m}{R_{bcc}^m}\right) \quad (1)$$

where V_i is the volume fraction of phase-*i*; $I_i^j(I_i^{hkl})$ is the integrated intensity for the {*hkl*} plane of phase-*i*; $R_i^j(R_i^{hkl})$ is the scattering factor which can be expressed as:

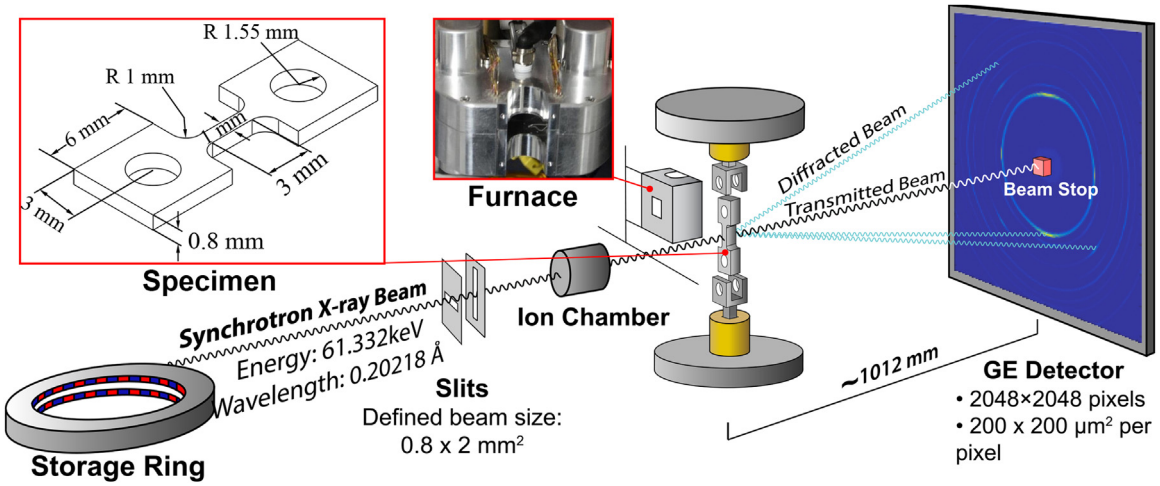

Fig. 1. Schematic illustration of the HEXRD setup for the in situ loading experiments. The furnace is movable and can be translated in and out of the x-ray beam path by a slide rail.